Micelles

Deutsche Ausgabe: DOI: 10.1002/ange.201604551
Internationale Ausgabe: DOI: 10.1002/anie.201604551

Monodisperse Cylindrical Micelles of Controlled Length with a Liquid-Crystalline Perfluorinated Core by 1D "Self-Seeding"

Xiaoyu Li, Bixin Jin, Yang Gao, Dominic W. Hayward, Mitchell A. Winnik, Yunjun Luo,* and Ian Manners**

Abstract: *Precise control over the morphology and dimensions of block copolymer (BCP) micelles has attracted interest due to the potential of this approach to generate functional nanostructures. Incorporation of liquid crystalline (LC) block can provide additional ways to vary micellar morphologies, but the formation of uniform micelles with controllable dimensions from LC BCPs has not yet been realized. Herein, we report the preparation of monodisperse cylindrical micelles with a LC poly(2-(perfluorooctyl)ethyl methacrylate (PFMA) core via a fragmentation-thermal annealing (F-TA) process, resembling the "self-seeding" process of crystalline BCP micelles. The average length of the cylinders increases with annealing temperature, with a narrow length distribution ($L_w/L_n < 1.1$). We also demonstrate the potential application of the cylinders with LC cores as a cargo-carrier by the successful incorporation of a hydrophobic fluorescent dye tagged with a fluorooctyl group.*

Over the past two decades, self-assembly of block copolymers (BCPs) in solution has offered an increasingly impressive and versatile bottom-up synthetic route to a wide variety of core–shell nanoparticles with well-defined shapes and functionalities.[1] Numerous methods have been developed to control the micellar morphologies, such as tuning the solvation environment,[2] the addition of small molecules,[3] variation of the BCP architectures,[4] and the introduction of crystalline[5] and liquid-crystalline (LC)[6] blocks. For LC BCPs in particular, the formation of a LC phase in the micellar core can provide additional possibilities to modify micellar morphologies.[6a–e] For example, Li and co-workers reported that the formation of a smectic phase in the wall of vesicular micelles led to the creation of faceted vesicles.[6b,c] In another report, Liu et al. prepared polygonal loop-like micelles, and demonstrated that the formation of sharp-angled vertices originated from the LC core.[6d] However, despite of the progress made, precise control over the morphologies and dimensions of LC BCP micelles is limited at present.

The living crystallization-driven self-assembly (CDSA) approach for amphiphilic crystalline BCPs has recently emerged as promising and versatile method to prepare 1D and 2D micellar structures in selective solvents.[5,7] In particular, living CDSA resembles a "living" covalent polymerization of molecular monomers, allowing access to well-defined micelles of predictable morphology and dimensions with substantial complexity.[5,7] This method has been utilized to prepare complex micelles from a variety of crystallizable BCPs[7c,d,8] and π-conjugated amphiphiles.[9,10]

In the living CDSA approach, key concepts are borrowed from polymer crystallization field, such as seeded growth and self-seeding. In a self-seeding process,[11] when polymer crystals containing regions with different crystallinity are heated above their apparent melting/dissolution temperatures, crystallites with higher crystallinity survive. Upon cooling, these surviving nuclei can initiate growth of those dissolved polymers, resulting in larger crystals.[12] This method can generate uniform polymeric crystals from homopolymers[13] and BCPs.[14] Recently, a 1D version of this method has been applied to crystalline BCPs, to produce monodisperse cylindrical micelles, via either temperature-induced or solvent-induced self-seeding route.[7b,d,15]

Herein, we report the preparation of monodisperse cylindrical micelles from a BCP with a LC core-forming block via a fragmentation-thermal annealing (F-TA) approach. We found that, though "self-seeding" processes are considered to be unique to crystalline materials, the average length of cylindrical micelles from a LC BCP increases with annealing temperatures in the F-TA process, resembling the "self-seeding" behavior of crystalline BCP micelles. Although the substrate-induced epitaxial growth of small LC molecules has been reported,[16] the "self-seeding" of LC materials has not been previously observed. We also show that these monodisperse cylindrical micelles can potentially be used as nanocarriers for hydrophobic cargo molecules.

The diblock copolymer $P2VP_{68}$-*b*-$PFMA_{41}$ was synthesized via sequential anionic polymerization (P2VP = poly(2-vinyl pyridine), PFMA = poly(2-(perfluorooctyl)ethyl methacrylate; the subscripts represent the number of repeating

[*] Prof. Dr. X. Y. Li, B. X. Jin, Prof. Dr. Y. J. Luo
School of Material Science and Technology
Beijing Institute of Technology
Beijing, 100081 (P.R. China)
E-mail: xiaoyuli@bit.edu.cn
yjluo@bit.edu.cn
D. W. Hayward, Prof. Dr. I. Manners
School of Chemistry
University of Bristol
Bristol BS8 1TS (UK)
E-mail: ian.manners@bristol.ac.uk
Dr. Y. Gao
School of Chemistry and Environment, Beihang University
Beijing, 100191 (P.R. China)
Prof. Dr. M. A. Winnik
Department of Chemistry, University of Toronto
Toronto, Ontario, M5S 3H6 (Canada)

Supporting information for this article can be found under: http://dx.doi.org/10.1002/anie.201604551.

units of each block). The polydispersity of the diblock copolymer was 1.12 (Figures S1 and S2, and in Table S1 in the Supporting Information). The formation of a smectic phase for PFMA homopolymer and PFMA-containing block copolymers and related materials has been well studied.[6d,e,17] Differential scanning calorimetry (DSC) analysis of the diblock copolymer revealed a smectic to isotropic phase transition at 84 °C (Figure S3(b)), close to the literature values for related BCPs.[6d,17] Wide angle X-ray scattering (WAXS) results from the P2VP-*b*-PFMA diblock copolymer was also in agreement with literature data (Figure S3(c)), suggesting the formation of an LC phase in the bulk.[6d,17]

Cylindrical micelles with a broad length distribution (the ratio between weight- and number-average lengths, $L_w/L_n > 2$, $L_n = 740$ nm) were obtained by directly dispersing the polymer in *iso*-propanol (*i*-PrOH) at 80 °C for 1 h, and then leaving the solution to cool to 23 °C, as shown by the transmission electron microscopy (TEM) image in Figure 1 a.

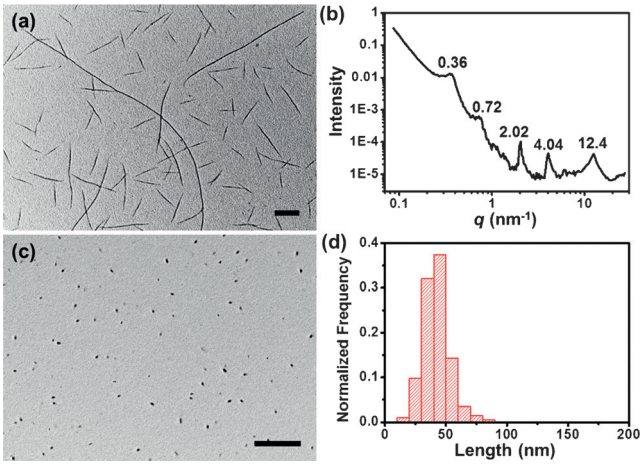

Figure 1. a) TEM images of the cylindrical micelles formed by dispersing $P2VP_{68}$-*b*-$PFMA_{41}$ into *i*-PrOH (0.5 mg mL^{-1}) at 80 °C for 1 h and cooling to 23 °C; b) spliced small, medium, and wide X-ray scattering spectra of dried cylindrical micelle sample shown in (a); c) the seeds obtained by ultrasonication of the cylindrical micelle solution in *i*-PrOH at 0 °C for 4 h; d) contour length distribution of the seeds in (c), $L_n = 42$ nm, $L_w = 45$ nm, $L_w/L_n = 1.07$. Scale bars are 500 nm.

In contrast, if the polymer was dispersed at lower temperatures, only random aggregates were produced (Figure S4). Since *i*-PrOH is selective for the P2VP block, the micelles consist of a P2VP corona and a PFMA core (Scheme 1 (I)). Due to the apparently higher mass density of the densely packed LC PFMA core, the micelles appeared as narrow width cylinders by TEM; the P2VP corona layer was only visible after staining with RuO_4 (Figure S5). The LC nature of the PFMA core of these cylindrical micelles was revealed by X-ray scattering spectra (Figure 1 b) on dried samples. The peak at $q = 0.36$ (and 0.72) nm^{-1} corresponds to a periodicity of 17.4 nm, which we assign to the diameter of the cylindrical micelles (ca. 18 nm based on TEM, see Figure S5); that at $q = 2.02$ (and 4.04) nm^{-1} corresponds to a long-range periodicity of 3.3 nm, originating from the average spacing between smectic layers in PFMA; and that at 12.4 nm^{-1} corresponds to a side-group spacing of 0.51 nm, in line with the value from the bulk sample (see Supporting Information pages S4–S5 and Scheme S1 for additional discussion).

Despite the presence of a LC rather than a crystalline core, monodisperse cylindrical micelles could be obtained if we performed F-TA procedures similar to those of "self-seeding" experiments. This involved two steps: in the first, the long and non-uniform cylindrical micelles (Figure 1 a) were fragmented by ultrasonication of a solution in *i*-PrOH at 0 °C for 4 h (Figure 1 c) to yield uniform short cylindrical micelles (seeds, Scheme 1 (II) A, $L_n = 42$ nm, $L_w/L_n = 1.07$). In a second step, longer uniform cylinders were obtained by thermal annealing of the seeds at desired temperatures between 35–75 °C (Scheme 1 (II) B). The lengths of the micelles were measured from TEM images, and the L_n, L_w and standard deviation (σ) were obtained. In the second step, aliquots of seed solutions were thermally annealed for 1 h in oil bath preset at desired temperatures, and then were allowed to gradually cool to 23 °C. For samples annealed at 50 °C and 75 °C (Figure 2 a,b), longer cylindrical micelles with narrow length distributions were obtained (for the sample annealed at 50 °C, $L_n = 146$ nm, $L_w/L_n = 1.07$; 75 °C, $L_n = 801$ nm, $L_w/L_n = 1.02$). The length information for samples at different annealing temperatures is summarized in Figure 2 c (also Figure S6–7 and Table S2). The length of the micelles increased with the annealing temperature, giving cylinders up to approximately 800 nm with a narrow length distribution ($L_w/L_n < 1.1$). Based on the initial length of the seeds and the final length of micelles after annealing, we calculated the fraction of surviving fragments at each annealing temperature. As shown in Figure 2 d, in the range of 35–75 °C, the fraction of surviving seeds decreased exponentially with increasing temperature, a key characteristic of a self-seeding process[11,15] (see Supporting Information page S6 for discussions).

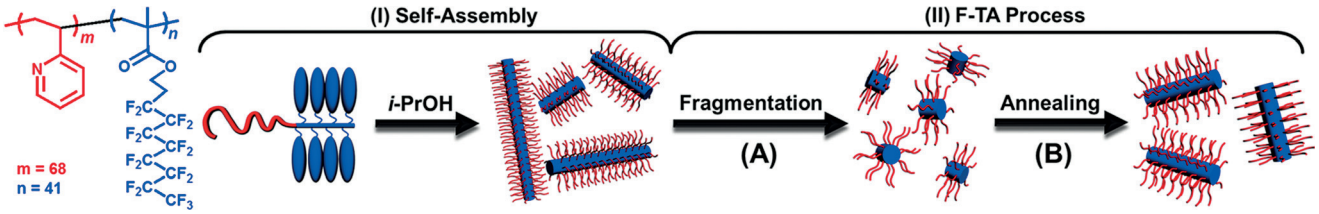

Scheme 1. Chemical Structure of P2VP-*b*-PFMA diblock copolymer. Schematic illustrations of I) the self-assembly process to form cylindrical micelles; and II) the F-TA process to prepare monodisperse micelles. See text for full details.

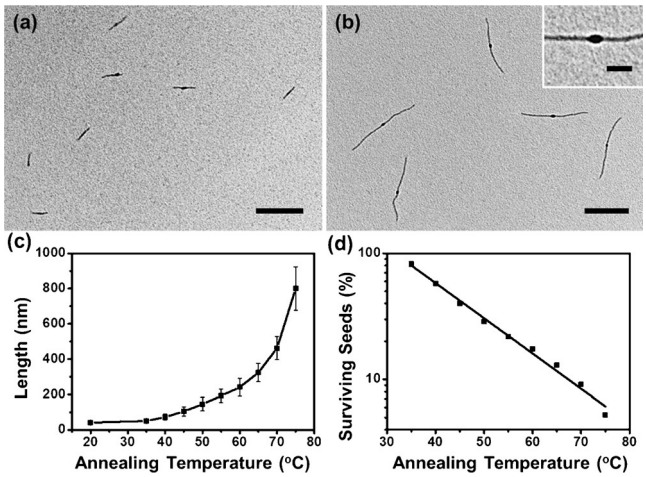

Figure 2. a,b) TEM images of the micelles obtained by annealing the seeds in *i*-PrOH at 0.1 mg mL^{-1} at a) 50 and b) 75 °C for 1 h, and cooling to 23 °C. Scale bars are 500 nm in the images and 100 nm in the inset. c) Number-average micelle length L_n versus annealing temperature (error bars are σ). d) Semi-logarithmic plots of fraction of surviving seeds in solution versus annealing temperatures. (The solid lines represent the best linear fits for the data points from 35 °C to 75 °C).

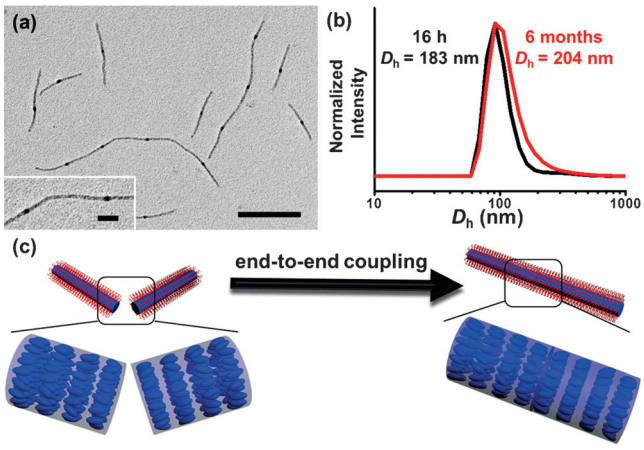

Figure 3. a) TEM image of cylindrical micelles that have undergone end-to-end coupling (cylindrical micelles prepared at a concentration of 0.2 mg mL^{-1} by annealing the seeds at 70 °C for 1 h, cooling to 23 °C, and aged for 6 months). Scale bar is 500 nm in the image and 100 nm in the inset. b) DLS data of the micelles characterized 16 h and 6 months after annealing at 70 °C. c) Schematic illustration of the end-to-end coupling process. In the expansion the corona chains and polymer backbones are removed for clarity, the blue ellipsoids represent the mesogenic perfluorooctyl groups in the PFMA core.

Several factors that might be expected to influence the observed micelle length were examined. Neither the solution concentration (Figure S8, Table S3) nor the annealing time (Figure S9 and Table S4) showed a significant effect on micelle length, as expected for a thermodynamical process.[15,18] After thermal annealing, the micelle length increased substantially in the initial 5 h after the sample was cooled to 23 °C and then remained constant after 8 h (Figure S10 and Table S5). In addition, the central dark segment of the cylindrical micelles (inset image in Figure 2b), corresponding to surviving seeds, appeared to be significantly darker by TEM. Moreover, when cylindrical micelles that were prepared by annealing at moderate temperatures (45, 55, 65 °C) were subsequently subject to a further annealing step at high temperature (75 °C), the resultant micelles were shorter than those prepared by direct thermal annealing at the same high temperature. Annealing below the smectic to isotropic phase transition temperature therefore appears to improve the degree of order in the core, leading to the dissolution of a smaller proportion of the seeds during the second heating process. The observed micelle length was found to decrease with increased temperature for the first annealing step (Figure S11 and Table S6), similar to a "self-seeding" process for crystalline BCP micelles.[7b,d,15]

Although the P2VP-*b*-PFMA BCP efficiently undergoes "self-seeding", attempts to induce controlled seeded-growth were unsuccessful. Even where significant growth was detected on addition of dissolved polymer to pre-existing cylindrical seeds at ambient or elevated temperatures, large numbers of new micelles were also generated under all conditions (see Figure S12 and Supporting Information pages S6–S7 for further discussion).

Interestingly, when the cylindrical micelles at high concentrations (e.g. 0.2 mg mL^{-1}) were aged for a long period, a significant percentage underwent end-to-end coupling based on TEM analysis (Figure 3a, Figure S13). The percentage population of cylindrical micelles underwent end-to-end coupling increased from 1 % (observed by TEM) in freshly annealed samples to 25 % after subsequent aging at 23 °C over 6 months. The original seeds used to generate the cylindrical micelles were also clearly resolved by TEM in the end-coupled micelles (Figure 3a). The length of the end-coupled micelles agreed well with that expected for integer multiples of the original monodisperse cylindrical micelles as building blocks. However, the actual connections between the cylindrical micelles showed no discerning features (Figure 3a inset). This finding clearly indicated the existence of end-to-end coupling mode in the micelle growth process.[19] Consistent with these observations, analysis by dynamic light scattering (DLS) showed that the apparent hydrodynamic diameter (D_h) and polydispersity (PDI) of the micelles increased after 6 months (Figure 3b), while the length of uncoupled micelles (measured from TEM images) remained unchanged (Table S7, see Supporting Information pages S7–S8 for additional analysis).

Several previous examples of the coupling of cylindrical micelles have been reported,[19,20] and this phenomenon has been attributed to the matching of their crystalline planes in the core,[19,20a] the presence of homopolymer corresponding to the core-forming block,[20b] removal of the corona,[20c] or covalent connection of the cylinders.[20d] In our case, this process is attributed to two factors (Figure 3c, see Supporting Information pages S7–S8 for additional discussion). First, the fluorinated FMA block is highly incompatible with hydrocarbon solvent, so that end-coupling of the cylindrical micelles would reduce the interfacial area resulting in a significant decrease in the overall free energy. Second, unlike the case of cylindrical micelles with a crystalline and

rigid core,[21] it is possible that the presence of a LC core does not require the same strict matching of crystalline planes for end-coupling[19] (see Figure 3c).

Similar to all symmetry-breaking materials, liquid crystals permit the existence of topological defects, which are regions of the order forced to be discontinuous.[22] The defects in LC structures have been used to direct molecular assembly,[22] organize nanoparticles,[23] gelate colloidal dispersions,[24] and template polymerization.[25] We therefore attempted to load solvophobic molecules inside the $P2VP_{68}$-*b*-$PFMA_{41}$ micelles. For this purpose, a BODIPY molecule containing a perfluorooctyl group (F-dye, Figure 4a, Figure S14,S15) was synthesized and used as the model cargo molecule.

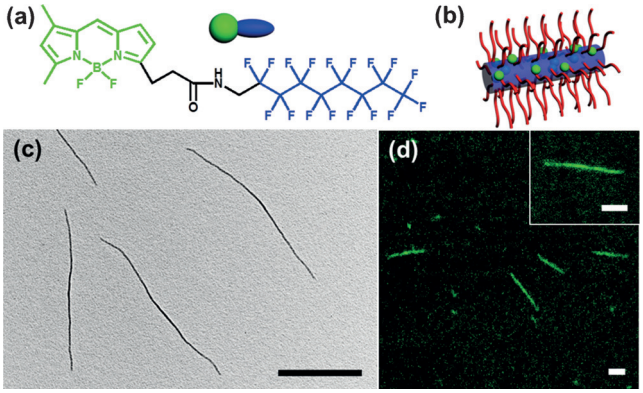

Figure 4. a) Chemical structure of F-dye. Schematic illustration (b), TEM (c), and LSCM (d) images of the loaded cylindrical micelles (0.1 mg mL^{-1}, F-dye loading ratio is 3 wt%), which were obtained by annealing the seeds with the F-dye at 80 °C for 1 h and cooling to 23 °C. Scale bars are 1 μm.

F-dye molecules were loaded by adding the solid to a dispersion of seeds ($L_n = 42$ nm, $L_w/L_n = 1.07$) in *i*-PrOH, annealing the resulting solution at 80 °C for 1 h, followed by slow cooling to 23 °C. Excess dye was removed via dialysis. As calculated from the UV/Vis absorbance, the loading ratio was 3% dye by mass (see Supporting Information pages S5–S6 for discussions). Figure 4c,d show the TEM and laser scanning confocal microscopy (LSCM) images of the loaded micelles, respectively. From TEM analysis (Figure 4c, Figure S16(a), Table S8), neither the micellar morphology nor the core diameter showed a noticeable change from the case of $P2VP_{68}$-*b*-$PFMA_{41}$ cylinders and an L_n value of 2155 nm ($L_w/L_n = 1.02$) was determined. LSCM clearly demonstrated the successful loading of F-dye molecules in the cylindrical micelles (Figure 4d). With a higher loading ratio (11% dye by mass), however, the cylindrical micelles became branched (Figure S16(b)) as the additional F-dye led to a thickening the cylindrical micelles in central middle section.[20c] The successful loading of F-dye was supported by spot energy dispersive X-ray (EDX) analysis (Figure S17). Dark field TEM images (Figure S18) also supported a thickening of the core in the central region of cylinders at high loading of F-dye.

In summary, we have demonstrated the successful preparation of monodisperse cylindrical micelles with controlled length from a LC block copolymer. Using a process that closely resembles the temperature-induced "self-seeding" route for crystalline BCP micelles, we could obtain uniform cylindrical micelles with lengths from 40 nm up to 800 nm. Furthermore, we could load dye molecules in the micelles to prepare cylindrical micelles loaded with cargo molecules, showing the potential application of these micelles as carriers for small hydrophobic molecules. These developments represent a significant advance toward the morphological control of LC BCP micelles, and demonstrate the wide applicability of the temperature-induced "self-seeding" method.

Acknowledgements

X.Y.L. acknowledges the EU for a Marie Curie Postdoctoral Fellowship. Y.G. and I.M. thank the EU for support. Y.G. thanks China Postdoctoral Science Foundation for a grant (2016M590029). The Ganesha X-ray scattering apparatus used for this research was purchased under EPSRC Grant "Atoms to Applications" Grant ref. EP/K035746/1. M.A.W. thanks NSERC for support. We also thank the Wolfson Bioimaging Facility at the University of Bristol for the use of the confocal microscopy facilities. This work is also supported by National Natural Science Foundation of China.

Keywords: block copolymers · cylindrical micelles · liquid crystalline · self-assembly · self-seeding

How to cite: *Angew. Chem. Int. Ed.* **2016**, *55*, 11392–11396
Angew. Chem. **2016**, *128*, 11564–11568

[1] a) Y. Y. Mai, A. Eisenberg, *Chem. Soc. Rev.* **2012**, *41*, 5969–5985; b) A. O. Moughton, M. A. Hillmyer, T. P. Lodge, *Macromolecules* **2012**, *45*, 2–19; c) F. H. Schacher, P. A. Rupar, I. Manners, *Angew. Chem. Int. Ed.* **2012**, *51*, 7898–7921; *Angew. Chem.* **2012**, *124*, 8020–8044; d) A. H. Gröschel, A. Walther, T. I. Löbling, F. H. Schacher, H. Schmalz, A. H. E. Müller, *Nature* **2013**, *503*, 247–251.

[2] a) Y. S. Yu, A. Eisenberg, *J. Am. Chem. Soc.* **1997**, *119*, 8383–8384; b) L. F. Zhang, A. Eisenberg, *Science* **1995**, *268*, 1728–1731; c) J. Dupont, G. J. Liu, K.-i. Niihara, R. Kimoto, H. Jinnai, *Angew. Chem. Int. Ed.* **2009**, *48*, 6144–6147; *Angew. Chem.* **2009**, *121*, 6260–6263.

[3] a) J. H. Zhu, S. Y. Zhang, K. Zhang, X. J. Wang, J. W. Mays, K. L. Wooley, D. J. Pochan, *Nat. Commun.* **2013**, *4*, 2297; b) H. G. Cui, Z. T. Chen, S. Zhong, K. L. Wooley, D. J. Pochan, *Science* **2007**, *317*, 647–650; c) D. J. Pochan, Z. Y. Chen, H. G. Cui, K. Hales, K. Qi, K. L. Wooley, *Science* **2004**, *306*, 94–97.

[4] Z. B. Li, E. Kesselman, Y. Talmon, M. A. Hillmyer, T. P. Lodge, *Science* **2004**, *306*, 98–101.

[5] a) X. S. Wang, G. Guérin, H. Wang, Y. S. Wang, I. Manners, M. A. Winnik, *Science* **2007**, *317*, 644–647; b) T. Gädt, N. S. Ieong, G. Cambridge, M. A. Winnik, I. Manners, *Nat. Mater.* **2009**, *8*, 144–150; c) Z. M. Hudson, C. E. Boott, M. E. Robinson, P. A. Rupar, M. A. Winnik, I. Manners, *Nat. Chem.* **2014**, *6*, 893–898; d) W. N. He, J. T. Xu, *Prog. Polym. Sci.* **2012**, *37*, 1350–1400; e) J. Schmelz, F. H. Schacher, H. Schmalz, *Soft Matter* **2013**, *9*, 2101–2107.

[6] a) J. Yang, D. Lévy, W. Deng, P. Keller, M.-H. Li, *Chem. Commun.* **2005**, 4345–4347; b) X. J. Xing, H. M. Shin, M. J. Bowick, Z. W. Yao, L. Jia, M.-H. Li, *Proc. Natl. Acad. Sci. USA* **2012**, *109*, 5202–5206; c) L. Jia, A. Cao, D. Lévy, B. Xu, P. A.

Albouy, X. J. Xing, M. J. Bowick, M.-H. Li, *Soft Matter* **2009**, *5*, 3446 – 3451; d) X. Y. Li, Y. Gao, X. J. Xing, G. J. Liu, *Macromolecules* **2013**, *46*, 7436 – 7442; e) Y. Gao, X. Y. Li, L. Z. Hong, G. J. Liu, *Macromolecules* **2012**, *45*, 1321 – 1330; f) H. L. Wu, L. Y. Zhang, Y. R. Xu, Z. Y. Ma, Z. H. Shen, X. H. Fan, Q. F. Zhou, *J. Polym. Sci. Part A* **2012**, *50*, 1792 – 1800; g) K. Skrabania, H. von Berlepsch, C. Böttcher, A. Laschewsky, *Macromolecules* **2010**, *43*, 271 – 281.

[7] a) J. B. Gilroy, T. Gädt, G. R. Whittell, L. Chabanne, J. M. Mitchels, R. M. Richardson, M. A. Winnik, I. Manners, *Nat. Chem.* **2010**, *2*, 566 – 570; b) J. S. Qian, G. Guérin, Y. J. Lu, G. Cambridge, I. Manners, M. A. Winnik, *Angew. Chem. Int. Ed.* **2011**, *50*, 1622 – 1625; *Angew. Chem.* **2011**, *123*, 1660 – 1663; c) J. Gwyther, J. B. Gilroy, P. Rupar, D. J. Lunn, E. Kynaston, S. K. Patra, G. Whittell, M. A. Winnik, I. Manners, *Chem. Eur. J.* **2013**, *19*, 9186 – 9197; d) J. S. Qian, X. Y. Li, D. J. Lunn, J. Gwyther, Z. M. Hudson, E. Kynaston, P. A. Rupar, M. A. Winnik, I. Manners, *J. Am. Chem. Soc.* **2014**, *136*, 4121 – 4124; e) H. B. Qiu, Z. M. Hudson, M. A. Winnik, I. Manners, *Science* **2015**, *347*, 1329 – 1332; f) X. Y. Li, Y. Gao, C. E. Boott, M. A. Winnik, I. Manners, *Nat. Commun.* **2015**, *6*, 8127.

[8] a) J. Schmelz, A. E. Schedl, C. Steinlein, I. Manners, H. Schmalz, *J. Am. Chem. Soc.* **2012**, *134*, 14217 – 14225; b) N. Petzetakis, A. P. Dove, R. K. O'Reilly, *Chem. Sci.* **2011**, *2*, 955 – 960; c) L. Sun, A. Pitto-Barry, N. Kirby, T. L. Schiller, A. M. Sanchez, M. A. Dyson, J. Sloan, N. R. Wilson, R. K. O'Reilly, A. P. Dove, *Nat. Commun.* **2014**, *5*, 5746.

[9] a) L. J. Bu, T. J. Dawson, R. C. Hayward, *ACS Nano* **2015**, *9*, 1878 – 1885; b) W. Zhang, W. Jin, T. Fukushima, A. Saeki, S. Seki, T. Aida, *Science* **2011**, *334*, 340 – 343; c) D. Görl, X. Zhang, V. Stepanenko, F. Würthner, *Nat. Commun.* **2015**, *6*, 7009; d) M. E. Robinson, D. J. Lunn, A. Nazemi, G. R. Whittell, L. De Cola, I. Manners, *Chem. Commun.* **2015**, *51*, 15921 – 15924; e) A. Aliprandi, M. Mauro, L. De Cola, *Nat. Chem.* **2015**, *8*, 10 – 15.

[10] S. Ogi, K. Sugiyasu, S. Manna, S. Samitsu, M. Takeuchi, *Nat. Chem.* **2014**, *6*, 188 – 195.

[11] J. J. Xu, Y. Ma, W. B. Hu, M. Rehahn, G. Reiter, *Nat. Mater.* **2009**, *8*, 348 – 353.

[12] D. C. Bassett, *Principles of Polymer Morphology*, University Press Cambridge, Cambridge, UK, **1981**.

[13] a) K. Rahimi, I. Botiz, N. Stingelin, N. Kayunkid, M. Sommer, F. P. V. Koch, N. Ha, O. Coulembier, P. Dubois, M. Brinkmann, G. Reiter, *Angew. Chem. Int. Ed.* **2012**, *51*, 11131 – 11135; *Angew. Chem.* **2012**, *124*, 11293 – 11297; b) B. Li, C. Y. Li, *J. Am. Chem. Soc.* **2007**, *129*, 12 – 13.

[14] a) M. S. Hsiao, J. X. Zheng, R. M. V. Horn, R. P. Quirk, E. L. Thomas, H. L. Chen, B. Lotz, S. Z. D. Cheng, *Macromolecules* **2009**, *42*, 8343 – 8352; b) W. H. Huang, C. X. Luo, J. L. Zhang, K. Yu, Y. C. Han, *Macromolecules* **2007**, *40*, 8022 – 8030.

[15] J. S. Qian, Y. J. Lu, A. Chia, M. Zhang, P. A. Rupar, N. Gunari, G. C. Walker, G. Cambridge, F. He, G. Guérin, I. Manners, M. A. Winnik, *ACS Nano* **2013**, *7*, 3754 – 3766.

[16] a) A. M. van de Craats, N. Stutzmann, O. Bunk, M. M. Nielsen, M. Watson, K. Müllen, H. D. Chanzy, H. Sirringhaus, R. H. Friend, *Adv. Mater.* **2003**, *15*, 495 – 499; b) B. O. Myrvold, *Liq. Cryst.* **1988**, *3*, 1255 – 1266.

[17] M. Al-Hussein, Y. Serero, O. Konovalov, A. Mourran, M. Moller, W. H. de Jeu, *Macromolecules* **2005**, *38*, 9610 – 9616.

[18] B. Lotz, A. J. Kovacs, *Kolloid Z. Z. Polym.* **1966**, *209*, 97 – 114.

[19] W. N. He, B. Zhou, J. T. Xu, B. Y. Du, Z. Q. Fan, *Macromolecules* **2012**, *45*, 9768 – 9778.

[20] a) J. X. Yang, B. Fan, J. H. Li, J. T. Xu, B. Y. Du, Z. Q. Fan, *Macromolecules* **2016**, *49*, 367 – 372; b) S. F. Mohd Yusoff, J. B. Gilroy, G. Cambridge, M. A. Winnik, I. Manners, *J. Am. Chem. Soc.* **2011**, *133*, 11220 – 11230; c) Y. Gao, H. B. Qiu, H. Zhou, X. Y. Li, R. Harniman, M. A. Winnik, I. Manners, *J. Am. Chem. Soc.* **2015**, *137*, 2203 – 2206; d) X. H. Yan, G. J. Liu, Z. Li, *J. Am. Chem. Soc.* **2004**, *126*, 10059 – 10066.

[21] J. B. Gilroy, P. A. Rupar, G. R. Whittell, L. Chabanne, N. J. Terrill, M. A. Winnik, I. Manners, R. M. Richardson, *J. Am. Chem. Soc.* **2011**, *133*, 17056 – 17062.

[22] X. G. Wang, D. S. Miller, E. Bukusoglu, J. J. de Pablo, N. L. Abbott, *Nat. Mater.* **2015**, *15*, 106 – 112.

[23] W. Dickson, G. A. Wurtz, P. R. Evans, R. J. Pollard, A. V. Zayats, *Nano Lett.* **2008**, *8*, 281 – 286.

[24] T. A. Wood, J. S. Lintuvuori, A. B. Schofield, D. Marenduzzo, W. C. K. Poon, *Science* **2011**, *334*, 79 – 83.

[25] H. Kikuchi, M. Yokota, Y. Hisakado, H. Yang, T. Kajiyama, *Nat. Mater.* **2002**, *1*, 64 – 68.

Received: May 10, 2016
Revised: July 2, 2016
Published online: August 11, 2016

